

Sample Selection with Uncertainty of Losses for Learning with Noisy Labels

Xiaobo Xia¹, Tongliang Liu¹, Bo Han²,
Mingming Gong³, Jun Yu⁴, Gang Niu⁵, Masashi Sugiyama^{5,6}

¹The University of Sydney; ²Hong Kong Baptist University;

³The University of Melbourne; ⁴University of Science and Technology of China;

⁵RIKEN; ⁶The University of Tokyo

Abstract

In learning with noisy labels, the *sample selection* approach is very popular, which regards *small-loss* data as correctly labeled during training. However, losses are generated on-the-fly based on the model being trained with noisy labels, and thus *large-loss* data are *likely but not certainly* to be incorrect. There are actually two possibilities of a large-loss data point: (a) it is mislabeled, and then its loss *decreases slower* than other data, since deep neural networks “learn patterns first”; (b) it belongs to an underrepresented group of data and *has not been selected yet*. In this paper, we incorporate the uncertainty of losses by adopting *interval estimation* instead of *point estimation* of losses, where lower bounds of the *confidence intervals* of losses derived from *distribution-free concentration inequalities*, but not losses themselves, are used for sample selection. In this way, we also give large-loss but less selected data a try; then, we can better distinguish between the cases (a) and (b) by seeing if the losses *effectively decrease* with the uncertainty after the try. As a result, we can better explore underrepresented data that are correctly labeled but seem to be mislabeled *at first glance*. Experiments demonstrate that the proposed method is superior to baselines and robust to a broad range of label noise types.

1 Introduction

Learning with noisy labels is one of the most challenging problems in weakly-supervised learning, since noisy labels are ubiquitous in the real world [40, 74, 45, 1, 70]. For instance, both crowd-sourcing and web crawling yield large numbers of noisy labels everyday [15]. Noisy labels can severely impair the performance of deep neural networks with strong memorization capacities [76, 78, 49, 34].

To reduce the influence of noisy labels, a lot of approaches have been recently proposed [43, 33, 35, 77, 80, 63, 64, 54, 37, 28, 38, 55, 69, 57, 22, 20, 17]. They can be generally divided into two main categories. The first one is to estimate the noise transition matrix [47, 52, 18, 14], which denotes the probabilities that clean labels flip into noisy labels. However, the noise transition matrix is hard to be estimated accurately, especially when the number of classes is large [74]. The second approach is sample selection, which is *our focus* in this paper. This approach is based on selecting possibly clean examples from a mini-batch for training [15, 71, 58, 74, 26, 58, 59]. Intuitively, if we can exploit less noisy data for network parameter updates, the network will be more robust.

A major question in sample selection is what *criteria* can be used to select possibly clean examples. At the present stage, the selection based on the *small-loss* criteria is the most common method, and has been verified to be effective in many circumstances [15, 19, 74, 60, 71]. Specifically, since deep networks *learn patterns first* [2], they would first memorize training data of clean labels and then those of noisy labels with the assumption that clean labels are of the majority in a noisy class. Small-loss examples can thus be regarded as clean examples *with high probability*. Therefore, in each iteration, prior methods [15, 60] select the small-loss examples based on *the predictions of the current network* for robust training.

However, such a selection procedure is *debatable*, since it arguably does *not consider uncertainty* in selection. The uncertainty comes from two aspects. First, this procedure has *uncertainty about small-loss examples*. Specifically, the procedure uses *limited time intervals* and only exploits the losses provided by the *current predictions*. For this reason, the estimation for the noisy class posterior is *unstable* [72], which causes the network predictions to be equally unstable. It thus *takes huge risks* to only use losses provided by the current predictions (Figure 1, left). Once wrong selection is made, the inferiority of accumulated errors will arise [74]. Second, this procedure has *uncertainty about large-loss examples*. To be specific, deep networks learn easy examples at the beginning of training, but ignore some clean examples with large losses. Nevertheless, such examples are always critical for generalization. For instance, when learning with *imbalanced* data, distinguishing the examples with *non-dominant labels* are more pivotal during training [39]. Deep networks often give large losses to such examples (Figure 1, right). Therefore, when learning under the realistic scenes, e.g., learning with noisy imbalanced data, prior sample selection methods cannot address such an issue well.

To relieve the above issues, we study the uncertainty of losses in the sample selection procedure to combat noisy labels. To reduce the uncertainty of small-loss examples, we extend time intervals and utilize the *mean* of training losses at different training iterations. In consideration of the bad influence of mislabeled data on training losses, we build two *robust mean estimators* from the perspectives of *soft truncation* and *hard truncation* w.r.t. the truncation level, respectively. Soft truncation makes the mean estimation more robust by *holistically* changing the behavior of losses. Hard truncation makes the mean estimation more robust by *locally* removing outliers from losses. To reduce the uncertainty of large-loss examples, we encourage networks to pick the sample that

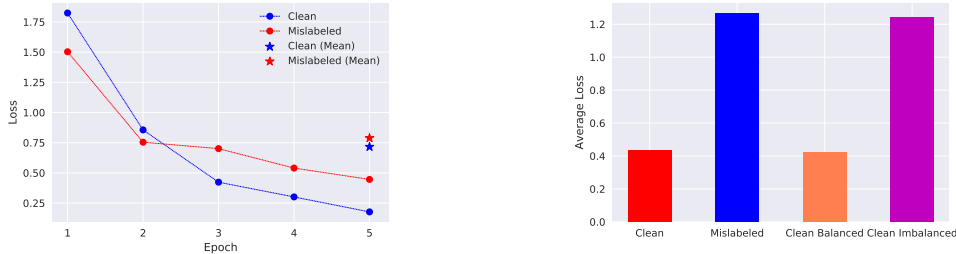


Figure 1: Illustrations of *uncertainty of losses*. Experiments are conducted on the imbalanced noisy *MNIST* dataset. **Left:** uncertainty of *small-loss* examples. At the beginning of training (Epochs 1 and 2), due to the instability of the current prediction, the network gives a larger loss to the clean example and does not select it for updates. If we consider the *mean* of training losses at different epochs, the clean example can be equipped with a smaller loss and then selected for updates. **Right:** uncertainty of *large-loss* examples. Since the deep network learns easy examples at the beginning of training, it gives a large loss to *clean imbalanced* data with non-dominant labels, which causes such data unable to be selected and severely influence generalization.

has not been selected in a conservative way. Furthermore, to address the two issues *simultaneously*, we derive *concentration inequalities* [5] for robust mean estimation and further employ statistical *confidence bounds* [3] to consider the number of times an example was selected during training.

The study of uncertainty of losses in learning with noisy labels can be justified as follows. In statistical learning, it is known that uncertainty is related to the quality of data [56]. Philosophically, we need *variety decrease* for selected data and *variety search* for unselected data, which share a common objective, i.e., *reduce the uncertainty of data to improve generalization* [42]. This is our original intention, since noisy labels could bring more uncertainty because of the low quality of noisy data. Nevertheless, due to the harm of noisy labels for generalization, we need to strike a good balance between variety decrease and search. Technically, our method is specially designed for handling noisy labels, which robustly uses network predictions and conservatively seeks less selected examples meanwhile to reduce the uncertainty of losses and then generalize well.

Before delving into details, we clearly emphasize our contributions in two folds. First, we reveal prior sample selection criteria in learning with noisy labels have some potential weaknesses and discuss them in detail. The new selection criteria are then proposed with detailed theoretical analyses. Second, we experimentally validate the proposed method on both synthetic noisy balanced/imbalanced datasets and real-world noisy datasets, on which it achieves superior robustness compared with the state-of-the-art methods in learning with noisy labels. The rest of the paper is organized as follows. In Section 2, we propose our robust learning paradigm step by step. Experimental results are discussed in Section 3. The conclusion is given in Section 4.

2 Method

In this section, we first introduce the problem setting and some background (Section 2.1). Then we discuss how to exploit training losses at different iterations (Section 2.2). Finally, we introduce the proposed method, which exploits training losses at different iterations more robustly and encourages networks to pick the sample that is less selected but could be correctly labeled (Section 2.3).

2.1 Preliminaries

Let \mathcal{X} and \mathcal{Y} be the input and output spaces. Consider a k -class classification problem, i.e., $\mathcal{Y} = [k]$, where $[k] = \{1, \dots, k\}$. In learning with noisy labels, the training data are all sampled from a corrupted distribution on $\mathcal{X} \times \mathcal{Y}$. We are given a sample with noisy labels, i.e., $\tilde{S} = \{(\mathbf{x}, \tilde{y})\}$, where \tilde{y} is the noisy label. The aim is to learn a robust classifier that could assign clean labels to test data by only exploiting a training sample with noisy labels.

Let $f : \mathcal{X} \rightarrow \mathbb{R}^k$ be the classifier with learnable parameters \mathbf{w} . At the i -th iteration during training, the parameters of the classifier f can be denoted as \mathbf{w}_i . Let $\ell : \mathbb{R}^k \times \mathcal{Y} \rightarrow \mathbb{R}$ be a *surrogate loss function* for k -class classification. We exploit the *softmax cross entropy loss* in this paper. Given an arbitrary training example (\mathbf{x}, \tilde{y}) , at the i -th iteration, we can obtain a loss ℓ_i , i.e., $\ell_i = \ell(f(\mathbf{w}_i; \mathbf{x}), \tilde{y})$. Hence, until the t -th iteration, we can obtain a training loss set L_t about the example (\mathbf{x}, \tilde{y}) , i.e., $L_t = \{\ell_1, \dots, \ell_t\}$.

In this paper, we assume that the training losses in L_t conform to a *Markov process*, which is to represent a changing system under the assumption that future states only depend on the current state (the Markov property) [51]. More specifically, at the i -th iteration, if we exploit an optimization algorithm for parameter updates (e.g., the stochastic gradient descent algorithm [4]) and omit other dependencies (e.g., \tilde{S}), we will have $P(\mathbf{w}_i | \mathbf{w}_{i-1}, \dots, \mathbf{w}_0) = P(\mathbf{w}_i | \mathbf{w}_{i-1})$, which means that the future state of the classifier f only depends on the current state. Furthermore, given a training example and the parameters of the classifier f , we can determine the loss of the training example as discussed. Therefore, the training losses in L_t will also conform to a Markov process.

2.2 Extended Time Intervals

As limited time interval cannot address the instability issue of the estimation for the noisy class posterior well [49], we extend time intervals and exploit the training losses at different training iterations for sample selection. One straightforward idea is to use the *mean* of training losses at different training iterations. Hence, the selection criterion could be

$$\tilde{\mu} = \frac{1}{t} \sum_{i=1}^t \ell_i. \quad (1)$$

It is intuitive and reasonable to use such a selection criterion for sample selection, since the operation of averaging can mitigate the risks caused by the unstable estimation for the noisy class posterior, following better generalization. Nevertheless, such a method could arguably achieve suboptimal classification performance for learning with noisy labels. The main reason is that, due to the great harm of mislabeled data, part of training losses are with too large uncertainty and could be seen as outliers. Therefore, it could be biased to use the mean of training losses consisting of such outliers [12], which further influences sample selection. More evaluations for our claims are provided in Section 3.

2.3 Robust Mean Estimation and Conservative Search

We extend time intervals and meanwhile exploit the training losses at different training iterations more robustly. Specifically, we build two robust mean estimators from the perspectives of *soft*

truncation and *hard truncation* [7]. Note that for specific tasks, it is feasible to decide the types of robust mean estimation with statistical tests based on some assumptions [8]. We leave the analysis as future work. Two *distribution-free* robust mean estimators are introduced as follows.

Soft truncation. We extend a classical M-estimator from [7] and exploit the *widest* possible choice of the *influence function*. More specifically, give a random variable X , let us consider a non-decreasing influence function $\psi : \mathbb{R} \rightarrow \mathbb{R}$ such that

$$\psi(X) = \log(1 + X + X^2/2), X \geq 0. \quad (2)$$

The choice of ψ is inspired by the *Taylor expansion of the exponential function*, which can make the estimation results more robust by reducing the side effect of extremum *holistically*. The illustration for this influence function is provided in Appendix A.1. For our task, given the observations on training losses, i.e., $L_t = \{\ell_1, \dots, \ell_t\}$, we estimate the mean robustly as follows:

$$\tilde{\mu}_s = \frac{1}{t} \sum_{i=1}^t \psi(\ell_i). \quad (3)$$

We term the above robust mean estimator (3) the *soft estimator*.

Hard truncation. We propose a new robust mean estimator based on hard truncation. Specifically, given the observations on training losses L_t , we first exploit the K-nearest neighbor (KNN) algorithm [30] to remove some underlying outliers in L_t . The number of outliers is denoted by t_o ($t_o < t$), which can be *adaptively determined* as discussed in [79]. Note that we can also employ other algorithms, e.g., principal component analysis [53] and the local outlier factor [6], to identify underlying outliers in L_t . The main reason we employ KNN is because of its relatively low computation costs [79].

The truncated loss observations on training losses are denoted by L_{t-t_o} . We then utilize L_{t-t_o} for the mean estimation. As the potential outliers are removed with high probability, the robustness of the estimation results will be enhanced. We denote such an estimated mean as $\tilde{\mu}_h$. We have

$$\tilde{\mu}_h = \frac{1}{t - t_o} \sum_{\ell_i \in L_{t-t_o}} \ell_i. \quad (4)$$

The corresponding estimator (4) is termed the *hard estimator*.

We derive concentration inequalities for the soft and hard estimators respectively. The search strategy for less selected examples and overall selection criterion are then provided. Note that we do not need to explicitly quantify the mean of training losses. We only need to sort the training examples based on the proposed selection criterion and then use the selected examples for robust training.

Theorem 1. Let $Z_n = \{z_1, \dots, z_n\}$ be an observation set with mean μ_z and variance σ^2 . By exploiting the non-decreasing influence function $\psi(z) = \log(1 + z + z^2/2)$. For any $\epsilon > 0$, we have

$$\left| \frac{1}{n} \sum_{i=1}^n \psi(z_i) - \mu_z \right| \leq \frac{\sigma^2(n + \frac{\sigma^2 \log(\epsilon^{-1})}{n^2})}{n - \sigma^2}, \quad (5)$$

with probability at least $1 - 2\epsilon$.

Proof can be found in Appendix A.1.

Theorem 2. Let $Z_n = \{z_1, \dots, z_n\}$ be a (not necessarily time homogeneous) Markov chain with mean μ_z , taking values in a Polish state space $\Lambda_1 \times \dots \times \Lambda_n$, and with a minimal mixing time τ_{\min} . The truncated set with hard truncation is denoted by Z_{n_o} , with $n_o < n$. If $|z_i|$ is upper bounded by Z . For any $\epsilon_1 > 0$ and $\epsilon_2 > 0$, we have

$$\left| \frac{1}{n - n_o} \sum_{z_i \in Z_n \setminus Z_{n_o}} -\mu_z \right| \leq \frac{1}{n - n_o} \left(2Z \sqrt{2\tau_{\min} \log \frac{2}{\epsilon_1}} + \frac{2Zn_o}{n} \sqrt{2\tau_{\min} \log \frac{2n}{\epsilon_2}} \right), \quad (6)$$

with probability at least $1 - \epsilon_1 - \epsilon_2$.

Proof can be found in Appendix A.2. For our task, let the training loss be upper-bounded by L . The value of L can be determined easily by training networks on noisy datasets and observing the loss distribution [1].

Conservative search and selection criteria. In this paper, we will use the concentration inequalities (5) and (6) to present conservative search and the overall sample selection criterion. Specifically, we exploit their *lower bounds* and consider the selected number of examples during training. The selection of the examples that are less selected is encouraged.

Denote the number of times one example was selected by $n_t (n_t \leq t)$. Let $\epsilon = \frac{1}{2t}$. For the circumstance with soft truncation, the selection criterion is

$$\ell_s^* = \tilde{\mu}_s - \frac{\sigma^2(t + \frac{\sigma^2 \log(2t)}{t^2})}{n_t - \sigma^2}. \quad (7)$$

Let $\epsilon_1 = \epsilon_2 = \frac{1}{2t}$, for the situation with hard truncation, by rewriting (6), the selection criterion is

$$\ell_h^* = \tilde{\mu}_h - \frac{2\sqrt{2\tau_{\min}}L(t + \sqrt{2}t_o)}{(t - t_o)\sqrt{t}} \sqrt{\frac{\log(4t)}{n_t}}. \quad (8)$$

Note that we directly replace t with n_t . If an example is rarely selected during training, n_t will be far less than n , which causes the lower bounds to change drastically. Hence, we do not use the mean of all training losses, but use the mean of training losses in fixed-length time intervals. More details about this can be checked in Section 3.

For the selection criteria (7) and (8), we can see that they consist of two terms and have one term with a minus sign. The first term in Eq. (7) (or Eq. (8)) is to reduce the uncertainty of small-loss examples, where we use robust mean estimation on training losses. The second term, i.e., the statistical confidence bound, is to encourage the network to choose the less selected examples (with a small n_t). The two terms are constraining and balanced with σ^2 or τ_{\min} . To avoid introducing strong assumptions on the underlying distribution of losses [8], we tune σ and τ_{\min} with a noisy validation set. For the mislabeled data, although the model has high uncertainties on them (i.e., a small n_t) and tends to pick them, the overfitting to the mislabeled data is harmful. Also, the mislabeled data and clean data are rather hard to distinguish in some cases as discussed. Thus, we should search underlying clean data in a conservative way. In this paper, we initialize σ and τ_{\min} with small values. This way can reduce the adverse effects of mislabeled data and meanwhile select the clean examples with large losses, which helps generalize. More evaluations will be presented in Section 3.

Algorithm 1 CNLCU Algorithm.

1: **Input** θ_1 and θ_2 , learning rate η , fixed τ , epoch T_k and T_{\max} , iteration t_{\max} ;
for $T = 1, 2, \dots, T_{\max}$ **do**
 2: **Shuffle** training dataset \tilde{S} ;
 for $t = 1, \dots, t_{\max}$ **do**
 3: **Fetch** mini-batch \bar{S} from \tilde{S} ;
 4: **Obtain** $\bar{S}_1 = \arg \min_{S': |S'| \geq R(T)|\bar{S}|} \ell^*(\theta_1, S')$; // calculated with Eq. (7) or Eq. (8)
 5: **Obtain** $\bar{S}_2 = \arg \min_{S': |S'| \geq R(T)|\bar{S}|} \ell^*(\theta_2, S')$; // calculated with Eq. (7) or Eq. (8)
 6: **Update** $\theta_1 = \theta_1 - \eta \nabla \ell(\theta_1, \bar{S}_2)$;
 7: **Update** $\theta_2 = \theta_2 - \eta \nabla \ell(\theta_2, \bar{S}_1)$;
 end
 8: **Update** $R(T) = 1 - \min \left\{ \frac{T}{T_k} \tau, \tau \right\}$;
end
9: **Output** θ_1 and θ_2 .

The overall procedure of the proposed method, which combats noisy labels by concerning uncertainty (CNLCU), is provided in Algorithm 1. CNLCU works in a mini-batch manner since all deep learning training methods are based on stochastic gradient descent. Following [15], we exploit two networks with parameters θ_1 and θ_2 respectively to teach each other. Specifically, when a mini-batch \bar{S} is formed (Step 3), we let two networks select a small proportion of examples in this mini-batch with Eq. (7) or (8) (Step 4 and Step 5). The number of instances is controlled by the function $R(T)$, and two networks only select $R(T)$ percentage of examples out of the mini-batch. The value of $R(T)$ should be larger at the beginning of training, and be smaller when the number of epochs goes large, which can make better use of memorization effects of deep networks [15] for sample selection. Then, the selected instances are fed into its peer network for parameter updates (Step 6 and Step 7).

3 Experiments

In this section, we evaluate the robustness of our proposed method to noisy labels with comprehensive experiments on the synthetic balanced noisy datasets (Section 3.1), synthetic imbalanced noisy datasets (Section 3.2), and real-world noisy dataset (Section 3.3).

3.1 Experiments on Synthetic Balanced Noisy Datasets

Datasets. We verify the effectiveness of our method on the manually corrupted version of the following datasets: *MNIST* [25], *F-MNIST* [66], *CIFAR-10* [24], and *CIFAR-100* [24], because these datasets are popularly used for the evaluation of learning with noisy labels in the literature [15, 74, 62, 26]. The four datasets are class-balanced. The important statistics of the used synthetic datasets are summarized in Appendix B.1.

Generating noisy labels. We consider broad types of label noise: (1). Symmetric noise (abbreviated as Sym.) [61, 35, 29]. (2) Asymmetric noise (abbreviated as Asym.) [36, 65, 60]. (3) Pairflip noise (abbreviated as Pair.) [15, 74, 80]. (4). Tridiagonal noise (abbreviated as Trid.) [77]. (5). Instance noise (abbreviated as Ins.) [10, 64]. The noise rate is set to 20% and 40% to ensure clean

labels are diagonally dominant [36]. More details about above noise are provided in Appendix B.1. We leave out 10% of noisy training examples as a validation set.

Baselines. We compare the proposed method (Algorithm 1) with following methods which focus on sample selection, and implement all methods with default parameters by PyTorch, and conduct all the experiments on NVIDIA Titan Xp GPUs. (1). S2E [71], which properly controls the sample selection process so that deep networks can better benefit from the memorization effects. (2). MentorNet [19], which learns a curriculum to filter out noisy data. We use self-paced MentorNet in this paper. (3). Co-teaching [15], which trains two networks simultaneously and cross-updates parameters of peer networks. (4). SIGUA [16], which exploits stochastic integrated gradient underweighted ascent to handle noisy labels. We use self-teaching SIGUA in this paper. (5). JoCor [60], which reduces the diversity of networks to improve robustness. Other types of baselines such as *adding regularization* are provided in Appendix B.2. Note that we do not compare the proposed method with some state-of-the-art methods, e.g., SELF [44] and DivideMix [27]. It is because their proposed methods are aggregations of multiple techniques. We mainly focus on sample selection in learning with noisy labels. Therefore, the comparison is not fair. Here, we term our methods with soft truncation and hard truncation as CNLCU-S and CNLCU-H respectively.

Network structure and optimizer. For *MNIST*, *F-MNIST*, and *CIFAR-10*, we use a 9-layer CNN structure from [15]. Due to the limited space, the experimental details on *CIFAR-100* are provided in Appendix B.3. All network structures we used here are standard test beds for weakly-supervised learning. For all experiments, the Adam optimizer [23] (momentum=0.9) is used with an initial learning rate of 0.001, and the batch size is set to 128 and we run 200 epochs. We linearly decay learning rate to zero from 80 to 200 epochs as did in [15]. We take two networks with the same architecture but different initializations as two classifiers as did in [15, 74, 60], since even with the same network and optimization method, different initializations can lead to different local optimal [15]. The details of network structures can be checked in Appendix C.

For the hyper-parameters σ^2 and τ_{\min} , we determine them in the range $\{10^{-1}, 10^{-2}, 10^{-3}, 10^{-4}\}$ with a noisy validation set. Here, we assume the noise level τ is known and set $R(T) = 1 - \min\{\frac{T}{T_k}\tau, \tau\}$ with $T_k=10$. If τ is not known in advanced, it can be inferred using validation sets [33, 75]. As for performance measurement, we use test accuracy, i.e., *test accuracy* = (# of correct prediction) / (# of testing). All experiments are repeated five times. We report the mean and standard deviation of experimental results.

Experimental results. The experimental results about test accuracy are provided in Table 1, 2, and 3. Specifically, for *MNIST*, as can be seen, our proposed methods, i.e., CNLCU-S and CNLCU-H, produce the best results in the vast majority of cases. In some cases such as asymmetric noise, the baseline S2E outperforms ours, which benefits the accurate estimation for the number of selected small-loss examples. For *F-MNIST*, the training data becomes complicated. S2E cannot achieve the accurate estimation in such situation and thus has no great performance like it got on *MNIST*. Our methods achieve varying degrees of lead over baselines. For *CIFAR-10*, our methods once again outperforms all the baseline methods. Although some baseline, e.g., Co-teaching, can work well in some cases, experimental results show that it cannot handle various noise types. In contrast, the proposed methods achieve superior robustness against broad noise types. The results mean that our methods can be better applied to actual scenarios, where the noise is diversiform.

Ablation study. We first conduct the ablation study to analyze the sensitivity of the length of time intervals. In order to *avoid too dense figures*, we exploit *MNIST* and *F-MNIST* with the

Noise type	Sym.		Asym.		Pair.		Trid.		Ins.	
	20%	40%	20%	40%	20%	40%	20%	40%	20%	40%
Method/Noise ratio	20%	40%	20%	40%	20%	40%	20%	40%	20%	40%
S2E	98.46 ± 0.06	95.62 ± 0.91	99.05 ± 0.02	98.45 ± 0.26	98.56 ± 0.32	94.22 ± 0.79	99.02 ± 0.09	97.23 ± 1.26	97.93 ± 1.26	94.02 ± 2.39
MentorNet	95.04 ± 0.03	92.08 ± 0.42	96.32 ± 0.17	90.86 ± 0.97	93.19 ± 0.17	90.93 ± 1.54	96.42 ± 0.09	93.28 ± 1.37	94.65 ± 0.73	90.11 ± 1.26
Co-teaching	97.53 ± 0.12	95.62 ± 0.30	98.25 ± 0.08	95.08 ± 0.43	96.05 ± 0.96	94.16 ± 1.37	98.05 ± 0.06	96.18 ± 0.85	97.96 ± 0.09	95.02 ± 0.39
SIGUA	92.31 ± 1.10	91.88 ± 0.92	93.96 ± 0.82	62.59 ± 0.15	93.77 ± 1.40	86.22 ± 1.75	94.92 ± 0.83	83.46 ± 2.98	92.90 ± 1.82	86.34 ± 3.51
JoCor	98.42 ± 0.14	98.04 ± 0.07	98.05 ± 0.37	94.55 ± 1.08	98.01 ± 0.19	96.85 ± 0.43	98.45 ± 0.17	96.98 ± 0.25	98.62 ± 0.06	96.07 ± 0.31
CNLCU-S	98.82 ± 0.03	98.31 ± 0.05	98.93 ± 0.06	97.67 ± 0.22	98.86 ± 0.06	97.71 ± 0.64	99.09 ± 0.04	98.02 ± 0.17	98.77 ± 0.08	97.78 ± 0.25
CNLCU-H	98.70 ± 0.06	98.24 ± 0.06	99.01 ± 0.04	98.01 ± 0.03	98.44 ± 0.19	97.37 ± 0.32	98.89 ± 0.15	97.92 ± 0.05	98.74 ± 0.16	97.42 ± 0.39

Table 1: Test accuracy (%) on *MNIST* over the last ten epochs. The best two results are in bold.

Noise type	Sym.		Asym.		Pair.		Trid.		Ins.	
	20%	40%	20%	40%	20%	40%	20%	40%	20%	40%
Method/Noise ratio	20%	40%	20%	40%	20%	40%	20%	40%	20%	40%
S2E	89.99 ± 2.07	75.32 ± 5.84	89.00 ± 0.95	81.03 ± 1.93	88.66 ± 1.32	67.09 ± 4.03	89.53 ± 2.63	77.29 ± 3.97	88.65 ± 2.12	79.35 ± 3.04
MentorNet	90.37 ± 0.17	86.53 ± 0.65	89.69 ± 0.19	67.21 ± 2.94	87.92 ± 1.08	83.70 ± 0.49	88.74 ± 0.33	85.63 ± 0.59	87.52 ± 0.15	83.27 ± 1.42
Co-teaching	91.48 ± 0.10	88.80 ± 0.29	91.03 ± 0.14	68.07 ± 4.58	90.77 ± 0.23	86.91 ± 0.71	91.24 ± 0.11	89.18 ± 0.36	90.60 ± 0.12	87.90 ± 0.45
SIGUA	87.64 ± 1.29	87.23 ± 0.72	76.97 ± 2.59	45.96 ± 3.40	69.59 ± 5.75	68.93 ± 2.80	79.97 ± 3.23	76.14 ± 4.24	76.92 ± 5.09	74.89 ± 4.84
JoCor	91.97 ± 0.13	89.96 ± 0.19	90.95 ± 0.21	79.79 ± 2.39	91.52 ± 0.24	87.40 ± 0.58	92.01 ± 0.17	89.42 ± 0.33	91.43 ± 0.71	87.59 ± 0.94
CNLCU-S	92.37 ± 0.15	91.45 ± 0.28	92.57 ± 0.15	83.14 ± 1.77	92.04 ± 0.26	88.20 ± 0.44	92.24 ± 0.17	90.08 ± 0.34	91.69 ± 0.10	89.02 ± 1.02
CNLCU-H	92.42 ± 0.21	91.60 ± 0.19	92.60 ± 0.18	82.69 ± 0.43	91.70 ± 0.18	87.70 ± 0.69	92.33 ± 0.26	90.22 ± 0.71	91.50 ± 0.21	88.79 ± 1.22

Table 2: Test accuracy on *F-MNIST* over the last ten epochs. The best two results are in bold.

mentioned noise settings as representative examples. For CNLCU-S, the length of time intervals is chosen in the range from 3 to 8. For CNLCU-H, the length of time intervals is chosen in the range from 10 to 15. Note that the reason for their different lengths is that their different mechanisms. Specifically, CNLCU-S holistically changes the behavior of losses, but does not remove any loss from the loss set. We thus do not need too long length of time intervals. As a comparison, CNLCU-H needs to remove some outliers from the loss set as discussed. The length should be longer to guarantee the number of examples available for robust mean estimation. The experimental results are provided in Appendix B.4, which show the proposed CNLCU-S and CNLCU-H are robust to the choices of the length of time intervals. Such robustness to hyperparameters means our methods can be applied in practice and does not need too much effect to tune the hyperparameters.

Furthermore, since our methods concern uncertainty from two aspects, i.e., the uncertainty

from both small-loss and large-loss examples, we conduct experiments to analyze each part of our methods. Also, as mentioned, we compare robust mean estimation with non-robust mean estimation when learning with noisy labels. More details are provided in Appendix B.4.

Noise type	Sym.		Asym.		Pair.		Trid.		Ins.	
	20%	40%	20%	40%	20%	40%	20%	40%	20%	40%
Method/Noise ratio										
S2E	80.78 ±0.88	69.72 ±3.94	84.03 ±1.01	75.04 ±1.24	81.72 ±0.93	61.50 ±4.63	81.44 ±0.59	64.39 ±2.82	79.89 ±0.26	62.42 ±3.11
MentorNet	80.92 ±0.48	74.67 ±1.17	80.37 ±0.26	71.69 ±1.06	77.98 ±0.31	69.39 ±1.73	78.02 ±0.29	71.56 ±0.93	77.02 ±0.71	68.17 ±2.52
Co-teaching	82.35 ±0.16	77.96 ±0.39	83.87 ±0.24	73.43 ±0.62	80.94 ±0.46	72.81 ±0.92	81.17 ±0.60	74.37 ±0.64	79.92 ±0.57	73.29 ±1.62
SIGUA	78.19 ±0.22	77.67 ±0.41	75.14 ±0.36	52.76 ±0.68	74.41 ±0.81	61.91 ±5.27	75.75 ±0.53	74.05 ±0.41	74.34 ±0.39	67.98 ±1.34
JoCor	80.96 ±0.25	76.65 ±0.43	81.39 ±0.74	69.92 ±1.63	80.33 ±0.20	71.62 ±1.05	79.03 ±0.13	74.33 ±1.09	78.21 ±0.34	71.46 ±1.27
CNLCU-S	83.03 ±0.21	78.25 ±0.70	85.06 ±0.17	75.34 ±0.32	83.16 ±0.25	73.19 ±1.25	82.77 ±0.32	74.37 ±1.37	82.03 ±0.37	73.67 ±1.09
CNLCU-H	83.03 ±0.47	78.33 ±0.50	84.95 ±0.27	75.29 ±0.80	83.39 ±0.68	73.40 ±1.53	82.52 ±0.71	74.79 ±1.13	81.93 ±0.25	73.58 ±1.39

Table 3: Test accuracy (%) on *CIFAR-10* over the last ten epochs. The best two results are in bold.

3.2 Experiments on Synthetic Imbalanced Noisy Datasets

Experimental setup. We exploit *MNIST* and *F-MNIST*. For these two datasets, we reduce the number of training examples along with the labels from “0” to “4” to 1% of previous numbers. We term such synthetic imbalanced noisy datasets as *IM-MNIST* and *IM-F-MNIST* respectively. This setting aims to simulate the extremely imbalanced circumstance, which is common in practice. Moreover, we exploit asymmetric noise, since these types of noise can produce more imbalanced case [47, 36]. Other settings such as the network structure and optimizer are the same as those in experiments on synthetic balanced noisy datasets.

As for performance measurements, we use test accuracy. In addition, we exploit the selected ratio of training examples with the imbalanced classes, i.e., $selected\ ratio = (\# \text{ of selected imbalanced labels} / \# \text{ of all selected labels})$. Intuitively, a higher selected ratio means the proposed method can make better use of training examples with the imbalanced classes, following better generalization [21].

Experimental results. The test accuracy achieved on *IM-MNIST* and *IM-F-MNIST* is presented in Figure 2. Recall the experimental results in Table 1 and 2, we can see that the imbalanced issue is *catastrophic* to the sample selection approach when learning with noisy labels. For *IM-MNIST*, as can be seen, all the baselines have serious overfitting in the early stages of training. The curves of test accuracy drop dramatically. As a comparison, the proposed CNLCU-S and CNLCU-H can give a try to large-loss but less selected data which are possible to be clean but equipped with imbalanced labels. Therefore, our methods always outperform baselines clearly. In the case of Asym. 10%, our methods achieve nearly 30% lead over baselines. For *IM-F-MNIST*, we can also see that our methods perform well and always achieve about 5% lead over all the baselines. Note that due to the huge challenge of this task, some baseline, e.g., S2E, has a large error bar. In addition,

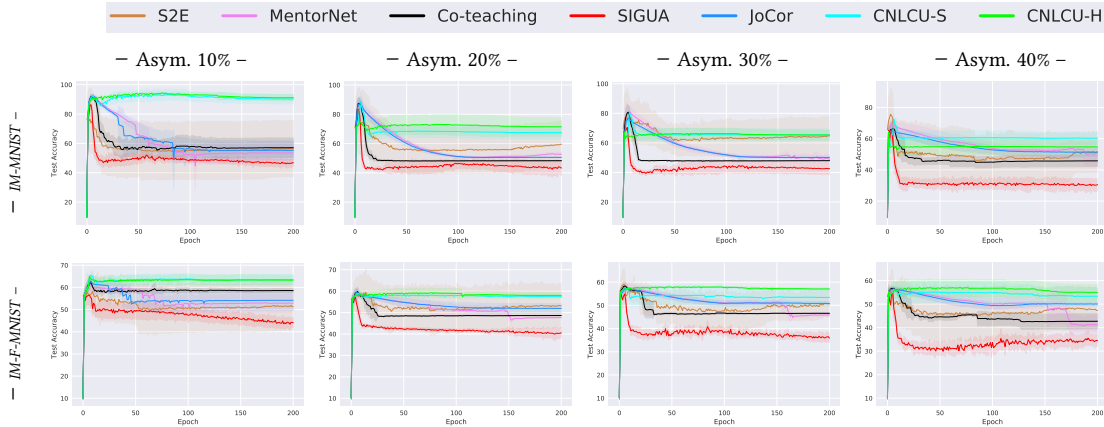


Figure 2: Test accuracy vs. number of epochs on *IM-MNIST* and *IM-F-MNIST*. The error bar for standard deviation in each figure has been shaded.

the baseline SIGUA performs badly. It is because SIGUA exploits stochastic integrated gradient underweighted ascent on large-loss examples, which makes the examples with imbalanced classes more difficult to be selected than them in other sample selection methods.

The selected ratio achieved on *IM-MNIST* and *IM-F-MNIST* is presented in Table 4. The results explain well why our methods perform better on synthetic imbalanced noisy datasets, i.e., our methods can make better use of training examples with the imbalanced classes. Note that since we give a try to large-loss but less selected data in a conservative way, the selected ratio is still far away from the class prior probability on the test set, i.e., 10%. However, a little improvement of the selection ratio can bring a considerable improvement of test accuracy. These results tell us that, in the sample selection approach when learning with noisy labels, improving the selected ratio of training examples with the imbalanced classes is challenging but promising for generalization. This practical problem deserves to be studied in depth.

Dataset	<i>IM-MNIST</i>				<i>IM-F-MNIST</i>			
	10%	20%	30%	40%	10%	20%	30%	40%
Method/Noise ratio	10%	20%	30%	40%	10%	20%	30%	40%
S2E	0.13 ± 0.12	0.11 ± 0.05	0.09 ± 0.02	0.05 ± 0.01	0.13 ± 0.04	0.17 ± 0.03	0.16 ± 0.02	0.12 ± 0.04
MentorNet	0.10 ± 0.02	0.15 ± 0.02	0.12 ± 0.03	0.13 ± 0.02	0.12 ± 0.01	0.15 ± 0.03	0.09 ± 0.01	0.14 ± 0.02
Co-teaching	0.09 ± 0.03	0.07 ± 0.02	0.05 ± 0.01	0.12 ± 0.01	0.17 ± 0.05	0.04 ± 0.00	0.13 ± 0.04	0.07 ± 0.01
SIGUA	0.04 ± 0.00	0.04 ± 0.00	0.01 ± 0.00	0.02 ± 0.00	0.03 ± 0.00	0.02 ± 0.00	0.04 ± 0.00	0.00 ± 0.00
JoCor	0.11 ± 0.04	0.08 ± 0.01	0.07 ± 0.03	0.06 ± 0.02	0.05 ± 0.01	0.13 ± 0.04	0.13 ± 0.03	0.07 ± 0.02
CNLCU-S	0.60 ± 0.11	0.37 ± 0.09	0.39 ± 0.04	0.38 ± 0.06	0.35 ± 0.03	0.39 ± 0.04	0.36 ± 0.03	0.30 ± 0.02
CNLCU-H	0.57 ± 0.13	0.32 ± 0.01	0.37 ± 0.07	0.32 ± 0.05	0.34 ± 0.02	0.35 ± 0.06	0.32 ± 0.04	0.28 ± 0.03

Table 4: Selected ratio (%) on *IM-MNIST* and *IM-F-MNIST*. The best two results are in bold.

3.3 Experiments on Real-world Noisy Datasets

Experimental setup. To verify the efficacy of our methods in the real-world scenario, we conduct experiments on the noisy dataset *Clothing1M* [67]. Specifically, for experiments on *Clothing1M*, we use the 1M images with noisy labels for training and 10k clean data for test respectively. Note that we do not use the 50k clean training data in all the experiments. For preprocessing, we resize the image to 256×256 , crop the middle 224×224 as input, and perform normalization. The experiments on *Clothing1M* are performed once due to the huge computational cost. We leave 10% noisy training data as a validation set for model selection. Note that we do not exploit the resampling trick during training [27]. Here, *Best* denotes the test accuracy of the epoch where the validation accuracy was optimal. *Last* denotes test accuracy of the last epoch. For the experiments on *Clothing1M*, we use a ResNet-18 pretrained on ImageNet as did in [60]. We also use the Adam optimizer and set the batch size to 64. During the training stage, we run 15 epochs in total and set the learning rate 8×10^{-4} , 5×10^{-4} , and 5×10^{-5} for 5 epochs each.

Experimental results. The results on *Clothing1M* are provided in Table 5. Specifically, the proposed methods get better results than state-of-the-art methods on *Best*, which achieve an improvement of +1.28% and +0.99% over the best baseline JoCor. Likewise, the proposed methods outperform all the baselines on *Last*. We achieve an improvement of +1.01% and +0.54% over JoCor. Note that the results are a bit lower than some state-of-art methods, e.g., [73] and [54], because of the following reasons. (1). We follow [60] and use ResNet-18 as a backbone. The state-of-art methods [73, 54] use ResNet-50 as a backbone. Our aim is to make the experimental results directly comparable with previous papers [60] in the same area. (2). We only focus on the sample selection approach and do not employ other advanced techniques, e.g., introducing the prior distribution [54] and combining semi-supervised learning [27, 44, 32].

Methods	S2E	MentorNet	Co-teaching	SIGUA	JoCor	CNLCU-S	CNLCU-H
<i>Best</i>	67.34	68.36	69.37	62.89	70.09	71.37	71.08
<i>Last</i>	65.90	67.42	68.62	58.73	69.75	70.76	70.29

Table 5: Test accuracy (%) on *Clothing1M*. The best two results are in bold.

4 Conclusion

In this paper, we focus on promoting the prior sample selection in learning with noisy labels, which starts from concerning the uncertainty of losses during training. We robustly use the training losses at different iterations to reduce the uncertainty of small-loss examples, and adopt confidence interval estimation to reduce the uncertainty of large-loss examples. Experiments are conducted on benchmark datasets, demonstrating the effectiveness of our method. We believe that this paper opens up new possibilities in the topics of using sample selection to handle noisy labels, especially in improving the robustness of models on imbalanced noisy datasets.

Acknowledgement

TL was supported by Australian Research Council Project DE-190101473. BH was supported by the RGC Early Career Scheme No. 22200720 and NSFC Young Scientists Fund No. 62006202. JY was supported by USTC Research Funds of the Double First-Class Initiative (YD2350002001). GN and MS were supported by JST AIP Acceleration Research Grant Number JPMJCR20U3, Japan. MS was also supported by the Institute for AI and Beyond, UTokyo.

A Proof of Theoretical Results

A.1 Proof of Theorem 1

For the circumstance with soft truncation, $\tilde{\mu}_z = \frac{1}{n} \sum_{i=1}^n \psi(z_i)$. As suggested in [7], we can exploit $\tilde{\mu}_z^-$ and $\tilde{\mu}_z^+$ such that

$$\tilde{\mu}_z^- \leq \tilde{\mu}_z \leq \tilde{\mu}_z^+, \quad (9)$$

to derive a bound for $\tilde{\mu}_z$. For some positive real parameter α , we define

$$r(\tilde{\mu}_z) = \sum_{i=1}^n \psi[\alpha(z_i - \tilde{\mu}_z)] = 0. \quad (10)$$

Let us introduce the quantity

$$r(\theta) = \frac{1}{\alpha n} \sum_{i=1}^n \psi[\alpha(z_i - \theta)]. \quad (11)$$

With the exponential moment inequality [13] and the C_r inequality [41], we have

$$\begin{aligned} \exp\{\alpha n r(\theta)\} &\leq \{1 + \alpha(\mu_z - \theta) + \alpha^2[\sigma^2 + (\mu_z - \theta)^2]\}^n \\ &\leq \exp\{n\alpha(\mu_z - \theta) + n\alpha^2[\sigma^2 + (\mu_z - \theta)^2]\}. \end{aligned} \quad (12)$$

In the same way,

$$\exp\{-\alpha n r(\theta)\} \leq \exp\{-n\alpha(\mu_z - \theta) + n\alpha^2[\sigma^2 + (\mu_z - \theta)^2]\}. \quad (13)$$

If we define for any $\mu_s \in \mathbb{R}$ the bounds

$$B_-(\theta) = \mu_z - \theta - \alpha[\sigma^2 + (\mu_z - \theta)^2] - \frac{\log(\epsilon^{-1})}{\alpha n} \quad (14)$$

and

$$B_+(\theta) = \mu_z - \theta + \alpha[\sigma^2 + (\mu_z - \theta)^2] + \frac{\log(\epsilon^{-1})}{\alpha n}. \quad (15)$$

From [9] (Lemma 2.2), we obtain that

$$P(r(\theta) > B_-(\theta)) \geq 1 - \epsilon \quad \text{and} \quad P(r(\theta) < B_+(\theta)) \geq 1 - \epsilon. \quad (16)$$

Let $\tilde{\mu}_z^-$ be the largest solution of the quadratic equation $B_-(\theta)$ and $\tilde{\mu}_z^+$ be the smallest solution of the quadratic equation $B_+(\theta)$. Also, to guarantee the solution of the quadratic equation, we assume

$$4\alpha^2\sigma^2 + \frac{4\log(\epsilon^{-1})}{n} \leq 1. \quad (17)$$

From [9] (Theorem 2.6), we then have

$$\tilde{\mu}_z^- \geq \mu_z - \frac{\alpha\sigma^2 + \frac{\log(\epsilon^{-1})}{\alpha n}}{\alpha - 1}, \quad (18)$$

and

$$\tilde{\mu}_z^+ \leq \mu_z + \frac{\alpha\sigma^2 + \frac{\log(\epsilon^{-1})}{\alpha n}}{\alpha - 1}. \quad (19)$$

With probability at least $1-2\epsilon$, we have $\tilde{\mu}_z^- \leq \tilde{\mu}_z \leq \tilde{\mu}_z^+$. We can choose $\alpha = \frac{n}{\sigma^2}$. Then we have

$$|\tilde{\mu}_z - \mu_z| \leq \frac{\sigma^2(n + \frac{\sigma^2 \log(\epsilon^{-1})}{n^2})}{n - \sigma^2}, \quad (20)$$

which holds with probability at least $1-2\epsilon$.

We exploit the lower bound and let $\epsilon = \frac{1}{2t}$. Then we have

$$\ell_s^* = \tilde{\mu}_s - \frac{\sigma^2(t + \frac{\sigma^2 \log(2t)}{t^2})}{n_t - \sigma^2}, \quad (21)$$

where n_t denotes the number of times that the example was selected in the time intervals.

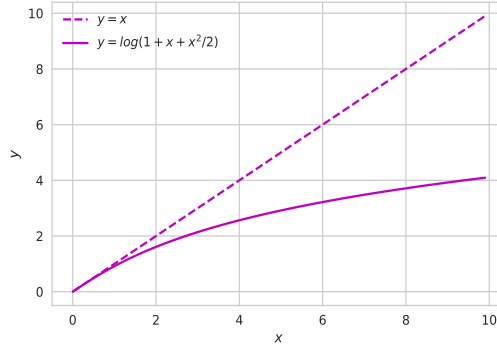


Figure 3: The illustration of the influence function for the soft estimator.

Here, we provide the graph of the used influence function for the soft estimator, which explains the mechanism of the function $y = \log(1 + x + x^2/2)$ more clearly. The illustration is presented in Figure 3. As can be seen, when x is large and may be an outlier, the influence function can reduce its negative impact for mean estimation. Therefore, we exploit such an influence function for robust mean estimation, which brings better classification performance.

A.2 Proof of Theorem 2

Lemma 1 ([48]). *Let $Z_n = \{z_1, \dots, z_n\}$ be a (not necessarily time homogeneous) Markov chain with mean μ_z , taking values in a Polish state space $\Lambda_1 \times \dots \times \Lambda_n$, with a mixing time $\tau(v)$ (for $0 \leq v \leq 1$). Let*

$$\tau_{\min} = \inf_{0 \leq v < 1} \tau(v) \cdot \left(\frac{2-v}{1-v} \right)^2. \quad (22)$$

For some $\eta \in \mathbb{R}^+$, suppose that $f : \Lambda \rightarrow \mathbb{R}$ satisfies the following inequality:

$$f(a) - f(b) \leq \sum_{i=1}^n \eta \mathbb{1}[a_i \neq b_i], \quad (23)$$

for every $a, b \in \Lambda$. Then for any $\epsilon \geq 0$, we have

$$P(|f(Z_n) - \mathbb{E}f(Z_n)| \geq \epsilon) \leq 2 \exp\left(\frac{-2\epsilon^2}{\eta^2 \tau_{\min}}\right). \quad (24)$$

The detailed definition of the mixing time for the Markov chain can be found in [48, 50]. Let f be the mean function. Following the prior work on mean estimation [31, 12, 11, 46], without loss of generality, we assume $\mu_z = 0$ for the underlying true distribution, and $|z_i|$ is upper bounded by Z . Then we can set η to $4Z/n$ for Eq. (23). Combining the above analyses, we can revise Eq. (24) as follows:

$$P\left(\left|\frac{1}{n} \sum_{i=1}^n z_i\right| \geq \frac{2Z}{n} \sqrt{2\tau_{\min} \log \frac{2}{\epsilon_1}}\right) \leq \epsilon_1, \quad (25)$$

and

$$P\left(\max_{i \in [n]} |z_i| \geq \frac{2Z}{n} \sqrt{2\tau_{\min} \log \frac{2n}{\epsilon_2}}\right) \leq \epsilon_2, \quad (26)$$

for $\epsilon_1 > 0$ and $\epsilon_2 > 0$. If we remove the potential outliers Z_{n_o} from Z_n . Therefore, we have

$$\begin{aligned} \left| \frac{1}{n - n_o} \sum_{z_i \in Z_n \setminus Z_{n_o}} - \mu_z \right| &= \frac{1}{n - n_o} \left| \sum_{z_i \in Z_n} - \sum_{z_i \in Z_{n_o}} \right| \\ &\leq \frac{1}{n - n_o} \left(\left| \sum_{z_i \in Z_n} \right| + \left| \sum_{z_i \in Z_{n_o}} \right| \right) \\ &\leq \frac{1}{n - n_o} \left(\left| \sum_{z_i \in Z_n} \right| + n_o \max_{i \in [n]} |z_i| \right) \\ &\leq \frac{1}{n - n_o} \left(2Z \sqrt{2\tau_{\min} \log \frac{2}{\epsilon_1}} + \frac{2Z n_o}{n} \sqrt{2\tau_{\min} \log \frac{2n}{\epsilon_2}} \right), \end{aligned} \quad (27)$$

which holds with probability at least $1 - \epsilon_1 - \epsilon_2$.

For our task, we exploit the concentration inequality. Let $\epsilon_1 = \epsilon_2 = \frac{1}{2t}$, and the losses be bounded by L . Next we can obtain

$$\begin{aligned}
|\tilde{\mu}_h - \mu| &\leq \frac{2L}{t - t_o} \left(\sqrt{2\tau_{\min} \log(4t)} + \frac{t_o}{t} \sqrt{4\tau_{\min} \log(4t)} \right) \\
&= \frac{2\sqrt{2\tau_{\min}}L(t + \sqrt{2}t_o)}{(t - t_o)t} \sqrt{\log(4t)}
\end{aligned} \tag{28}$$

with the probability at least $1 - \frac{1}{t}$. In practice, it is easy to identify the value of L . For example, we can training deep networks on noisy datasets to observe the loss distributions. Then, we exploit the lower bound such that

$$\ell_h^* = \tilde{\mu}_h - \frac{2\sqrt{2\tau_{\min}}L(t + \sqrt{2}t_o)}{(t - t_o)\sqrt{t}} \sqrt{\frac{\log(4t)}{n_t}} \tag{29}$$

for sample selection.

B Complementary Experimental Analyses

	# of training	# of testing	# of class	size
<i>MNIST</i>	60,000	10,000	10	$28 \times 28 \times 1$
<i>F-MNIST</i>	60,000	10,000	10	$28 \times 28 \times 1$
<i>CIFAR-10</i>	50,000	10,000	10	$32 \times 32 \times 3$
<i>CIFAR-100</i>	50,000	10,000	100	$32 \times 32 \times 3$

Table 6: Summary of synthetic datasets used in the experiments.

B.1 The Details of Datasets and Generating Noisy Labels

For the details of datasets, the important statistics of the used datasets are summarized in Table 6.

For the details of generating noisy labels, we exploit both *class-dependent* and *instance-dependent label noise* which include five types of synthetic label noise to verify the effectiveness of the proposed method. Here, we describe the details of the noise setting as follows:

(1). Class-dependent label noise:

- Symmetric noise: this kind of label noise is generated by flipping labels in each class uniformly to incorrect labels of other classes.
- Asymmetric noise : this kind of label noise is generated by flipping labels within a set of similar classes. In this paper, for *MNIST*, flipping $2 \rightarrow 7$, $3 \rightarrow 8$, $5 \leftrightarrow 6$. For *F-MNIST*, flipping TSHIRT \rightarrow SHIRT, PULLOVER \rightarrow COAT, SANDALS \rightarrow SNEAKER. For *CIFAR-10*, flipping TRUCK \rightarrow AUTOMOBILE, BIRD \rightarrow AIRPLANE, DEER \rightarrow HORSE, CAT \leftrightarrow DOG. For *CIFAR-100*, the 100 classes are grouped into 20 super-classes, and each has 5 sub-classes. Each class is then flipped into the next within the same super-class.
- Pairflip noise: the noise flips each class to its adjacent class.
- Tridiagonal noise: the noise corresponds to a spectral of classes where adjacent classes are easier to be mutually mislabeled, unlike the unidirectional pair flipping. It can be implemented by two consecutive pair flipping transformations in the opposite direction.

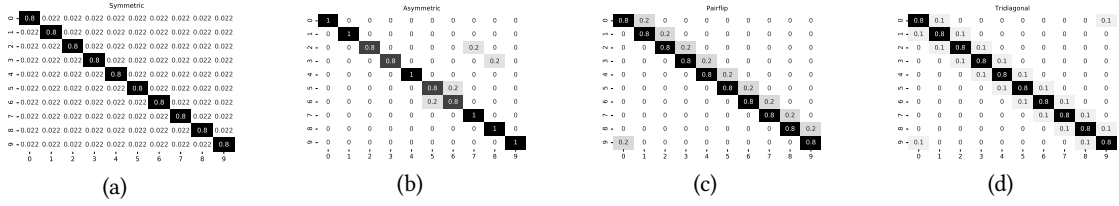


Figure 4: Synthetic class-dependent transition matrices used in our experiments on *MNIST*. The noise rate is set to 20%.

Noise type	Sym.		Asym.		Pair.		Trid.		Ins.	
	20%	40%	20%	40%	20%	40%	20%	40%	20%	40%
Method/Noise ratio	20%	40%	20%	40%	20%	40%	20%	40%	20%	40%
APL	98.76	94.92	98.63	88.65	98.66	68.44	98.93	76.44	97.63	87.90
	± 0.06	± 0.31	± 0.05	± 1.72	± 0.10	± 2.95	± 0.04	± 3.04	± 0.73	± 1.94
CDR	94.77	92.16	96.73	91.05	93.25	71.02	94.06	70.28	93.17	77.45
	± 0.17	± 0.73	± 0.19	± 0.76	± 0.90	± 3.89	± 0.92	± 4.01	± 0.96	± 3.04

Table 7: Test accuracy (%) on *MNIST* over the last ten epochs.

Noise type	Sym.		Asym.		Pair.		Trid.		Ins.	
	20%	40%	20%	40%	20%	40%	20%	40%	20%	40%
Method/Noise ratio	20%	40%	20%	40%	20%	40%	20%	40%	20%	40%
APL	91.73	89.06	90.13	80.34	90.22	78.54	90.84	86.53	90.96	85.55
	± 0.20	± 0.41	± 0.17	± 0.63	± 0.80	± 4.33	± 0.22	± 0.76	± 0.77	± 2.86
CDR	85.62	71.83	89.78	79.05	85.72	69.07	86.75	73.63	85.92	73.14
	± 0.96	± 1.37	± 0.41	± 1.39	± 0.65	± 2.31	± 1.19	± 2.82	± 1.43	± 3.12

Table 8: Test accuracy on *F-MNIST* over the last ten epochs.

(2). Instance-dependent label noise:

- Instance noise: the noise is quite realistic, where the probability that an instance is mislabeled depends on its features. We generate this type of label noise to validate the effectiveness of the proposed method as did in [64].

We use synthetic noisy *MNIST* as an example and plot the noise transition matrices in Figure 4. The noise rate is set to 20%.

B.2 Comparison with Other Types of Baselines

As we focus on the sample selection approach in learning with noisy labels, in the main paper (Section 3.1), we fairly compare our methods with the baselines which also focus on sample selection. Here, we evaluate other types of baselines. We exploit APL [36] and CDR [65], which add implicit regularization from different perspectives. The experiments are conducted on *MNIST* and *F-MNIST*. Other experimental settings are the same as those in the main paper. The experimental results are provided in Table 7 and 8, which show that the proposed methods can outperform them with respect to classification performance.

B.3 Experiments on Synthetic *CIFAR-100*

For *CIFAR-100*, we use a 7-layer CNN structure from [74, 71]. Other experimental settings are the same as those in the experiments on *MNIST*, *F-MNIST*, and *CIFAR-10*. The results are provided in Table 9. We can see the proposed method outperforms all the baselines.

Noise type	Sym.		Asym.		Pair.		Trid.		Ins.	
Method/Noise ratio	20%	40%	20%	40%	20%	40%	20%	40%	20%	40%
S2E	44.59 ±0.32	25.78 ±5.44	42.18 ±1.73	26.81 ±2.25	42.99 ±1.54	26.96 ±2.48	43.16 ±0.93	27.72 ±3.56	43.13 ±0.67	27.12 ±3.86
MentorNet	43.15 ±0.42	37.62 ±0.89	41.03 ±0.22	28.27 ±0.41	40.06 ±0.37	27.17 ±0.92	42.20 ±0.30	31.74 ±0.88	40.54 ±0.69	33.09 ±1.53
Co-teaching	45.17 ±0.25	40.95 ±0.52	42.76 ±0.34	30.27 ±0.33	42.50 ±0.39	30.07 ±0.17	44.41 ±0.41	34.96 ±0.35	42.23 ±0.52	35.87 ±1.47
SIGUA	42.03 ±0.33	40.53 ±0.49	36.67 ±0.25	26.71 ±0.42	36.48 ±0.37	26.73 ±0.33	39.21 ±0.40	32.69 ±0.36	39.19 ±0.32	33.51 ±0.43
JoCor	45.93 ±0.21	41.56 ±0.57	42.89 ±0.37	29.19 ±1.42	42.12 ±0.35	30.12 ±0.65	44.98 ±0.27	34.23 ±1.13	44.28 ±0.59	35.60 ±0.99
CNLCU-S	46.09 ±0.29	42.11 ±0.70	43.06 ±0.28	30.47 ±0.37	43.08 ±0.92	30.33 ±0.74	45.19 ±0.90	35.49 ±1.30	44.80 ±0.70	36.23 ±0.49
CNLCU-H	46.27 ±0.38	42.05 ±0.87	43.21 ±0.93	30.55 ±0.72	43.25 ±0.75	30.79 ±0.86	45.02 ±1.06	35.24 ±0.93	45.02 ±1.07	36.17 ±1.54

Table 9: Test accuracy (%) on *CIFAR-100* over the last ten epochs. The best two results are in bold.

B.4 Experiments for Ablation Study

We conduct the ablation study to analyze the sensitivity of the length of time intervals. The results are shown in Figure 5 and 6. As we can see, the proposed method, i.e., CNLCU-S and CNLCU-H are robust to the choices of hyperparameters.

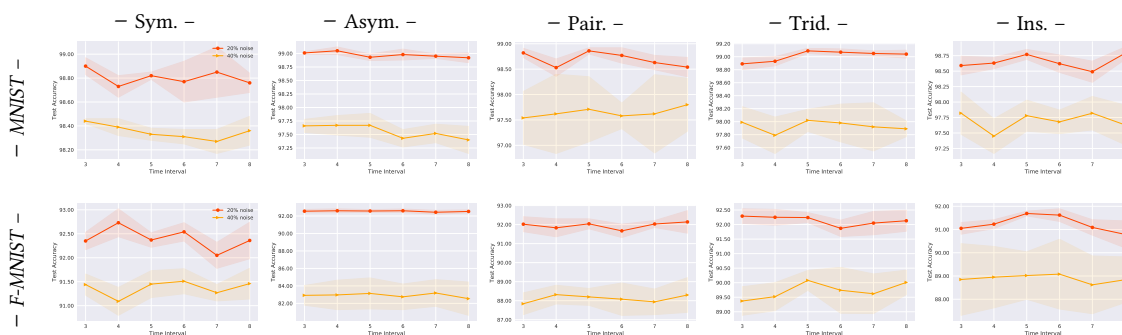


Figure 5: Illustrations of the hyperparameter sensitivity for the proposed CNLCU-S. The error bar for standard deviation in each figure has been shaded.

Note that in this paper, we concern uncertainty from *two aspects*, i.e., the uncertainty about small-loss examples and the uncertainty about large-loss examples. Here, we conduct ablation study to show the effect of removing different components to provide insights into what makes

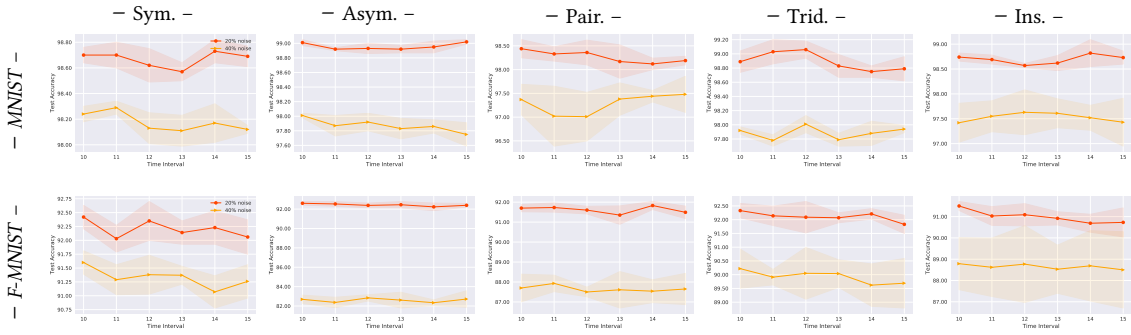


Figure 6: Illustrations of the hyperparameter sensitivity for the proposed CNLCU-H. The error bar for standard deviation in each figure has been shaded.

the proposed methods successful. The experiments are conducted on *MNIST* and *F-MNIST*. Other experimental settings are the same as those in the main paper (Section 3.1). Note that we employ two networks to teach each other following [15]. Therefore, when we do not consider uncertainty in sample selection, the proposed methods will *reduce to* the baseline Co-teaching [15].

To study the effect of concerning uncertainty about small-loss examples, we remove the concerns about large-loss examples, i.e., the network is not encouraged to choose the less selected examples for updates. We express such a setting as “without concerning about large-loss examples” (abbreviated as *w/o cl*). To study the effect of concerning uncertainty about large-loss examples, we remove the concerns about small-loss examples, i.e., we only exploit the predictions of the current network. We express such a setting as “without concerning about small-loss examples” (abbreviated as *w/o cs*). Besides, we express the setting which directly uses non-robust mean as Co-teaching-M.

The experimental results of ablation study are provided in Table 10 and 11. As can be seen, both aspects of uncertainty concerns can improve the robustness of models. Therefore, combining two uncertainty concerns, we can better combat noisy labels. In addition, robust mean estimation is superior to the non-robust mean in learning with noisy labels.

C Complementary Explanation for Network Structures

Table 12 describes the 9-layer CNN [15] used on *MNIST*, *F-MNIST*, and *CIFAR-10*. Table 13 describes the 9-layer CNN [74] used on *CIFAR-100*. Here, LReLU stands for Leaky ReLU [68]. The slopes of all LReLU functions in the networks are set to 0.01. Note that that the 7/9-layer CNN is a standard and common practice in weakly supervised learning. We decided to use these CNNs, since then the experimental results are directly comparable with previous approaches in the same area, i.e., learning with noisy labels.

Noise type	Sym.		Asym.		Pair.		Trid.		Ins.	
	20%	40%	20%	40%	20%	40%	20%	40%	20%	40%
Method/Noise ratio										
CNLCU-S	98.82 ±0.03	98.31 ±0.05	98.93 ±0.06	97.67 ±0.22	98.86 ±0.06	97.71 ±0.64	99.09 ±0.04	98.02 ±0.17	98.77 ±0.08	97.78 ±0.25
CNLCU-S <i>w/o cl</i>	98.02 ±0.08	96.83 ±0.29	98.50 ±0.04	96.25 ±0.13	98.22 ±0.13	96.08 ±0.75	98.64 ±0.31	97.25 ±0.24	98.17 ±0.20	97.13 ±0.40
CNLCU-S <i>w/o cs</i>	98.15 ±0.20	97.12 ±0.22	98.36 ±0.07	96.39 ±0.48	98.04 ±0.24	96.12 ±0.68	98.74 ±0.05	97.30 ±0.52	98.11 ±0.15	97.32 ±0.43
CNLCU-H	98.70 ±0.06	98.24 ±0.06	99.01 ±0.04	98.01 ±0.03	98.44 ±0.19	97.37 ±0.32	98.89 ±0.15	97.92 ±0.05	98.74 ±0.16	97.42 ±0.39
CNLCU-H <i>w/o cl</i>	98.06 ±0.13	96.92 ±0.23	98.39 ±0.04	96.51 ±0.57	97.04 ±0.87	95.62 ±0.93	98.33 ±0.47	97.41 ±0.92	98.01 ±0.20	96.15 ±0.28
CNLCU-H <i>w/o cs</i>	98.19 ±0.22	97.05 ±0.49	98.76 ±0.59	97.17 ±0.60	97.26 ±1.19	96.31 ±0.25	98.29 ±0.17	97.65 ±0.92	98.34 ±0.36	96.49 ±0.48
Co-teaching-M	97.72 ±0.08	97.78 ±0.32	98.27 ±0.03	95.42 ±0.42	96.22 ±0.10	95.01 ±0.65	97.92 ±0.14	96.64 ±0.77	98.02 ±0.04	96.03 ±0.57
Co-teaching	97.53 ±0.12	95.62 ±0.30	98.25 ±0.08	95.08 ±0.43	96.05 ±0.96	94.16 ±1.37	98.05 ±0.06	96.18 ±0.85	97.96 ±0.09	95.02 ±0.39

Table 10: Test accuracy (%) on *MNIST* over last ten epochs.

Noise type	Sym.		Asym.		Pair.		Trid.		Ins.	
	20%	40%	20%	40%	20%	40%	20%	40%	20%	40%
Method/Noise ratio										
CNLCU-S	92.37 ±0.15	91.45 ±0.28	92.57 ±0.15	83.14 ±1.77	92.04 ±0.26	88.20 ±0.44	92.24 ±0.17	90.08 ±0.34	91.69 ±0.10	89.02 ±1.02
CNLCU-S <i>w/o cl</i>	91.77 ±0.35	89.40 ±0.26	91.25 ±0.30	72.93 ±2.63	91.53 ±0.17	87.31 ±0.59	91.31 ±0.52	89.50 ±0.32	91.09 ±0.13	88.45 ±0.57
CNLCU-S <i>w/o cs</i>	91.85 ±0.33	90.76 ±0.28	91.94 ±0.09	80.99 ±2.74	91.28 ±0.20	87.31 ±0.72	91.39 ±0.07	89.29 ±0.51	90.98 ±0.43	88.73 ±0.62
CNLCU-H	92.42 ±0.21	91.60 ±0.19	92.60 ±0.18	82.69 ±0.43	91.70 ±0.18	87.70 ±0.69	92.33 ±0.26	90.22 ±0.71	91.50 ±0.21	88.79 ±1.22
CNLCU-H <i>w/o cl</i>	91.70 ±0.04	90.05 ±0.31	91.08 ±0.06	71.35 ±2.30	91.03 ±0.29	87.22 ±0.72	91.59 ±0.07	90.01 ±0.24	90.80 ±0.27	88.31 ±1.09
CNLCU-H <i>w/o cs</i>	91.82 ±0.13	90.92 ±0.42	92.45 ±0.25	80.73 ±1.63	91.21 ±0.17	87.49 ±0.32	92.08 ±0.13	89.72 ±0.24	91.21 ±0.38	88.62 ±0.73
Co-teaching-M	91.33 ±0.18	89.05 ±0.73	91.14 ±0.90	71.03 ±3.73	90.85 ±0.61	86.95 ±0.19	91.50 ±0.46	89.18 ±0.44	90.74 ±1.06	88.25 ±0.92
Co-teaching	91.48 ±0.10	88.80 ±0.29	91.03 ±0.14	68.07 ±4.58	90.77 ±0.23	86.91 ±0.71	91.24 ±0.11	89.18 ±0.36	90.60 ±0.12	87.90 ±0.45

Table 11: Test accuracy (%) on *F-MNIST* over last ten epochs.

Table 12: CNN on *MNIST*, *F-MNIST*, and *CIFAR-10*.

CNN on <i>MNIST</i>	CNN on <i>F-MNIST</i>	CNN on <i>CIFAR-10</i>
28×28 Gray Image	28×28 Gray Image	32×32 RGB Image
	3×3 conv, 128 LReLU	
	3×3 conv, 128 LReLU	
	3×3 conv, 128 LReLU	
	2×2 max-pool	
	dropout, $p = 0.25$	
	3×3 conv, 256 LReLU	
	3×3 conv, 256 LReLU	
	3×3 conv, 256 LReLU	
	2×2 max-pool	
	dropout, $p = 0.25$	
	3×3 conv, 512 LReLU	
	3×3 conv, 256 LReLU	
	3×3 conv, 128 LReLU	
	avg-pool	
dense 128→10	dense 128→10	dense 128→10

Table 13: CNN on *CIFAR-100*.

CNN on <i>CIFAR-100</i>
32×32 RGB Image
3×3 conv, 64 ReLU
3×3 conv, 64 ReLU
2×2 max-pool
3×3 conv, 128 ReLU
3×3 conv, 128 ReLU
2×2 max-pool
3×3 conv, 196 ReLU
3×3 conv, 196 ReLU
2×2 max-pool
dense 256→100

References

- [1] Eric Arazo, Diego Ortego, Paul Albert, Noel O’Connor, and Kevin McGuinness. Unsupervised label noise modeling and loss correction. In *ICML*, pages 312–321, 2019.
- [2] Devansh Arpit, Stanisław Jastrzębski, Nicolas Ballas, David Krueger, Emmanuel Bengio, Maxinder S Kanwal, Tegan Maharaj, Asja Fischer, Aaron Courville, Yoshua Bengio, et al. A closer look at memorization in deep networks. In *ICML*, pages 233–242, 2017.
- [3] Peter Auer. Using confidence bounds for exploitation-exploration trade-offs. *Journal of Machine Learning Research*, 3(Nov):397–422, 2002.
- [4] Léon Bottou. Stochastic gradient descent tricks. In *Neural networks: Tricks of the trade*, pages 421–436. Springer, 2012.
- [5] Stéphane Boucheron, Gábor Lugosi, and Pascal Massart. *Concentration inequalities: A nonasymptotic theory of independence*. Oxford university press, 2013.
- [6] Markus M Breunig, Hans-Peter Kriegel, Raymond T Ng, and Jörg Sander. Lof: identifying density-based local outliers. In *SIGMOD*, pages 93–104, 2000.
- [7] Olivier Catoni. Challenging the empirical mean and empirical variance: a deviation study. In *Annales de l’IHP Probabilités et statistiques*, volume 48, pages 1148–1185, 2012.
- [8] Arijit Chakrabarty and Gennady Samorodnitsky. Understanding heavy tails in a bounded world or, is a truncated heavy tail heavy or not? *Stochastic models*, 28(1):109–143, 2012.
- [9] Peng Chen, Xinghu Jin, Xiang Li, and Lihu Xu. A generalized catoni’s m -estimator under finite α -th moment assumption with $\alpha \in (1, 2)$. *arXiv preprint arXiv:2010.05008*, 2020.

- [10] Jiacheng Cheng, Tongliang Liu, Kotagiri Ramamohanarao, and Dacheng Tao. Learning with bounded instance-and label-dependent label noise. In *ICML, 2020*.
- [11] Ilias Diakonikolas and Daniel M Kane. Recent advances in algorithmic high-dimensional robust statistics. *arXiv preprint arXiv:1911.05911*, 2019.
- [12] Ilias Diakonikolas, Daniel M Kane, and Ankit Pensia. Outlier robust mean estimation with subgaussian rates via stability. *arXiv preprint arXiv:2007.15618*, 2020.
- [13] Evarist Giné, Rafał Latała, and Joel Zinn. Exponential and moment inequalities for u-statistics. In *High Dimensional Probability II*, pages 13–38. Springer, 2000.
- [14] Bo Han, Jiangchao Yao, Gang Niu, Mingyuan Zhou, Ivor Tsang, Ya Zhang, and Masashi Sugiyama. Masking: A new perspective of noisy supervision. In *NeurIPS*, pages 5836–5846, 2018.
- [15] Bo Han, Quanming Yao, Xingrui Yu, Gang Niu, Miao Xu, Weihua Hu, Ivor Tsang, and Masashi Sugiyama. Co-teaching: Robust training of deep neural networks with extremely noisy labels. In *NeurIPS*, pages 8527–8537, 2018.
- [16] Bo Han, Gang Niu, Xingrui Yu, Quanming Yao, Miao Xu, Ivor Tsang, and Masashi Sugiyama. Sigua: Forgetting may make learning with noisy labels more robust. In *ICML*, pages 4006–4016, 2020.
- [17] Hrayr Harutyunyan, Kyle Reing, Greg Ver Steeg, and Aram Galstyan. Improving generalization by controlling label-noise information in neural network weights. In *ICML*, pages 4071–4081, 2020.
- [18] Dan Hendrycks, Mantas Mazeika, Duncan Wilson, and Kevin Gimpel. Using trusted data to train deep networks on labels corrupted by severe noise. In *NeurIPS*, 2018.
- [19] Lu Jiang, Zhengyuan Zhou, Thomas Leung, Li-Jia Li, and Li Fei-Fei. MentorNet: Learning data-driven curriculum for very deep neural networks on corrupted labels. In *ICML*, pages 2309–2318, 2018.
- [20] Lu Jiang, Di Huang, Mason Liu, and Weilong Yang. Beyond synthetic noise: Deep learning on controlled noisy labels. In *ICML*, pages 4804–4815, 2020.
- [21] Bingyi Kang, Saining Xie, Marcus Rohrbach, Zhicheng Yan, Albert Gordo, Jiashi Feng, and Yannis Kalantidis. Decoupling representation and classifier for long-tailed recognition. In *ICLR*, 2020.
- [22] Youngdong Kim, Junho Yim, Juseung Yun, and Junmo Kim. Nlnl: Negative learning for noisy labels. In *ICCV*, pages 101–110, 2019.
- [23] Diederik P Kingma and Jimmy Ba. Adam: A method for stochastic optimization. *arXiv preprint arXiv:1412.6980*, 2014.
- [24] Alex Krizhevsky. Learning multiple layers of features from tiny images. Technical report, 2009.

- [25] Yann LeCun, Corinna Cortes, and Christopher J.C. Burges. The MNIST database of handwritten digits. <http://yann.lecun.com/exdb/mnist/>.
- [26] Kimin Lee, Sukmin Yun, Kibok Lee, Honglak Lee, Bo Li, and Jinwoo Shin. Robust inference via generative classifiers for handling noisy labels. In *ICML*, pages 3763–3772, 2019.
- [27] Junnan Li, Richard Socher, and Steven C.H. Hoi. Dividemix: Learning with noisy labels as semi-supervised learning. In *ICLR*, 2020.
- [28] Mingchen Li, Mahdi Soltanolkotabi, and Samet Oymak. Gradient descent with early stopping is provably robust to label noise for overparameterized neural networks. In *AISTATS*, 2020.
- [29] Xuefeng Li, Tongliang Liu, Bo Han, Gang Niu, and Masashi Sugiyama. Provably end-to-end label-noise learning without anchor points. 2021.
- [30] Yihua Liao and V Rao Vemuri. Use of k-nearest neighbor classifier for intrusion detection. *Computers & security*, 21(5):439–448, 2002.
- [31] Liu Liu, Tianyang Li, and Constantine Caramanis. High dimensional robust m-estimation: Arbitrary corruption and heavy tails. *arXiv preprint arXiv:1901.08237*, 2019.
- [32] Sheng Liu, Jonathan Niles-Weed, Narges Razavian, and Carlos Fernandez-Granda. Early-learning regularization prevents memorization of noisy labels. In *NeurIPS*, 2020.
- [33] Tongliang Liu and Dacheng Tao. Classification with noisy labels by importance reweighting. *IEEE Transactions on pattern analysis and machine intelligence*, 38(3):447–461, 2016.
- [34] Michal Lukasik, Srinadh Bhojanapalli, Aditya Menon, and Sanjiv Kumar. Does label smoothing mitigate label noise? In *ICML*, pages 6448–6458, 2020.
- [35] Xingjun Ma, Yisen Wang, Michael E Houle, Shuo Zhou, Sarah M Erfani, Shu-Tao Xia, Sudanthi Wijewickrema, and James Bailey. Dimensionality-driven learning with noisy labels. In *ICML*, pages 3361–3370, 2018.
- [36] Xingjun Ma, Hanxun Huang, Yisen Wang, Simone Romano, Sarah Erfani, and James Bailey. Normalized loss functions for deep learning with noisy labels. In *ICML*, pages 6543–6553, 2020.
- [37] Eran Malach and Shai Shalev-Shwartz. Decoupling" when to update" from" how to update". In *NeurIPS*, pages 960–970, 2017.
- [38] Aditya Krishna Menon, Brendan Van Rooyen, and Nagarajan Natarajan. Learning from binary labels with instance-dependent noise. *Machine Learning*, 107(8-10):1561–1595, 2018.
- [39] Aditya Krishna Menon, Sadeep Jayasumana, Ankit Singh Rawat, Himanshu Jain, Andreas Veit, and Sanjiv Kumar. Long-tail learning via logit adjustment. *arXiv preprint arXiv:2007.07314*, 2020.
- [40] Baharan Mirzasoleiman, Kaidi Cao, and Jure Leskovec. Coresets for robust training of neural networks against noisy labels. In *NeurIPS*, 2020.

- [41] Mehryar Mohri, Afshin Rostamizadeh, and Ameet Talwalkar. *Foundations of Machine Learning*. MIT Press, 2018.
- [42] David S Moore. Uncertainty. *On the shoulders of giants: New approaches to numeracy*, pages 95–137, 1990.
- [43] Nagarajan Natarajan, Inderjit S Dhillon, Pradeep K Ravikumar, and Ambuj Tewari. Learning with noisy labels. In *NeurIPS*, pages 1196–1204, 2013.
- [44] Duc Tam Nguyen, Chaithanya Kumar Mummadi, Thi Phuong Nhung Ngo, Thi Hoai Phuong Nguyen, Laura Beggel, and Thomas Brox. Self: Learning to filter noisy labels with self-ensembling. In *ICLR*, 2020.
- [45] Kento Nishi, Yi Ding, Alex Rich, and Tobias Höllerer. Augmentation strategies for learning with noisy labels. *arXiv preprint arXiv:2103.02130*, 2021.
- [46] Laura Niss and Ambuj Tewari. What you see may not be what you get: Ucb bandit algorithms robust to ϵ -contamination. In *UAI*, pages 450–459, 2020.
- [47] Giorgio Patrini, Alessandro Rozza, Aditya Krishna Menon, Richard Nock, and Lizhen Qu. Making deep neural networks robust to label noise: A loss correction approach. In *CVPR*, pages 1944–1952, 2017.
- [48] Daniel Paulin et al. Concentration inequalities for markov chains by marton couplings and spectral methods. *Electronic Journal of Probability*, 20, 2015.
- [49] Geoff Pleiss, Tianyi Zhang, Ethan R Elenberg, and Kilian Q Weinberger. Identifying mislabeled data using the area under the margin ranking. In *NeurIPS*, 2020.
- [50] Gareth O Roberts, Jeffrey S Rosenthal, et al. General state space markov chains and mcmc algorithms. *Probability surveys*, 1:20–71, 2004.
- [51] Jeffrey S Rosenthal. Faithful couplings of markov chains: now equals forever. *Advances in Applied Mathematics*, 18(3):372–381, 1997.
- [52] Jun Shu, Qian Zhao, Zengben Xu, and Deyu Meng. Meta transition adaptation for robust deep learning with noisy labels. *arXiv preprint arXiv:2006.05697*, 2020.
- [53] Mei-Ling Shyu, Shu-Ching Chen, Kanoksri Sarinnapakorn, and LiWu Chang. A novel anomaly detection scheme based on principal component classifier. Technical report, 2003.
- [54] Daiki Tanaka, Daiki Ikami, Toshihiko Yamasaki, and Kiyoharu Aizawa. Joint optimization framework for learning with noisy labels. In *CVPR*, 2018.
- [55] Kiran K Thekumparampil, Ashish Khetan, Zinan Lin, and Sewoong Oh. Robustness of conditional gans to noisy labels. In *NeurIPS*, pages 10271–10282, 2018.
- [56] Vladimir Vapnik. *The nature of statistical learning theory*. Springer science & business media, 2013.

- [57] Qizhou Wang, Jiangchao Yao, Chen Gong, Tongliang Liu, Mingming Gong, Hongxia Yang, and Bo Han. Learning with group noise. In *AAAI*, 2021.
- [58] Xiaobo Wang, Shuo Wang, Jun Wang, Hailin Shi, and Tao Mei. Co-mining: Deep face recognition with noisy labels. In *ICCV*, pages 9358–9367, 2019.
- [59] Yisen Wang, Weiyang Liu, Xingjun Ma, James Bailey, Hongyuan Zha, Le Song, and Shu-Tao Xia. Iterative learning with open-set noisy labels. In *CVPR*, pages 8688–8696, 2018.
- [60] Hongxin Wei, Lei Feng, Xiangyu Chen, and Bo An. Combating noisy labels by agreement: A joint training method with co-regularization. In *CVPR*, pages 13726–13735, 2020.
- [61] Pengxiang Wu, Songzhu Zheng, Mayank Goswami, Dimitris Metaxas, and Chao Chen. A topological filter for learning with label noise. In *NeurIPS*, 2020.
- [62] Songhua Wu, Xiaobo Xia, Tongliang Liu, Bo Han, Mingming Gong, Nannan Wang, Haifeng Liu, and Gang Niu. Class2simi: A noise reduction perspective on learning with noisy labels. In *ICML*, 2021.
- [63] Xiaobo Xia, Tongliang Liu, Nannan Wang, Bo Han, Chen Gong, Gang Niu, and Masashi Sugiyama. Are anchor points really indispensable in label-noise learning? In *NeurIPS*, pages 6835–6846, 2019.
- [64] Xiaobo Xia, Tongliang Liu, Bo Han, Nannan Wang, Mingming Gong, Haifeng Liu, Gang Niu, Dacheng Tao, and Masashi Sugiyama. Part-dependent label noise: Towards instance-dependent label noise. In *NeurIPS*, 2020.
- [65] Xiaobo Xia, Tongliang Liu, Bo Han, Chen Gong, Nannan Wang, Zongyuan Ge, and Yi Chang. Robust early-learning: Hindering the memorization of noisy labels. In *ICLR*, 2021.
- [66] Han Xiao, Kashif Rasul, and Roland Vollgraf. Fashion-mnist: a novel image dataset for benchmarking machine learning algorithms. *arXiv preprint arXiv:1708.07747*, 2017.
- [67] Tong Xiao, Tian Xia, Yi Yang, Chang Huang, and Xiaogang Wang. Learning from massive noisy labeled data for image classification. In *CVPR*, pages 2691–2699, 2015.
- [68] Bing Xu, Naiyan Wang, Tianqi Chen, and Mu Li. Empirical evaluation of rectified activations in convolutional network. *arXiv preprint arXiv:1505.00853*, 2015.
- [69] Yilun Xu, Peng Cao, Yuqing Kong, and Yizhou Wang. L_dmi: A novel information-theoretic loss function for training deep nets robust to label noise. In *NeurIPS*, pages 6222–6233, 2019.
- [70] Shuo Yang, Lu Liu, and Min Xu. Free lunch for few-shot learning: Distribution calibration. In *ICLR*, 2021.
- [71] Quanming Yao, Hansi Yang, Bo Han, Gang Niu, and James Tin-Yau Kwok. Searching to exploit memorization effect in learning with noisy labels. In *ICML*, pages 10789–10798, 2020.
- [72] Yu Yao, Tongliang Liu, Bo Han, Mingming Gong, Jiankang Deng, Gang Niu, and Masashi Sugiyama. Dual t: Reducing estimation error for transition matrix in label-noise learning. In *NeurIPS*, 2020.

- [73] Kun Yi and Jianxin Wu. Probabilistic end-to-end noise correction for learning with noisy labels. In *CVPR*, pages 7017–7025, 2019.
- [74] Xingrui Yu, Bo Han, Jiangchao Yao, Gang Niu, Ivor W Tsang, and Masashi Sugiyama. How does disagreement benefit co-teaching? In *ICML*, 2019.
- [75] Xiyu Yu, Tongliang Liu, Mingming Gong, Kayhan Batmanghelich, and Dacheng Tao. An efficient and provable approach for mixture proportion estimation using linear independence assumption. In *CVPR*, pages 4480–4489, 2018.
- [76] Chiyuan Zhang, Samy Bengio, Moritz Hardt, Benjamin Recht, and Oriol Vinyals. Understanding deep learning requires rethinking generalization. In *ICLR*, 2017.
- [77] Yivan Zhang, Gang Niu, and Masashi Sugiyama. Learning noise transition matrix from only noisy labels via total variation regularization. In *ICML*, 2021.
- [78] Zhilu Zhang and Mert Sabuncu. Generalized cross entropy loss for training deep neural networks with noisy labels. In *NeurIPS*, pages 8778–8788, 2018.
- [79] Yue Zhao, Zain Nasrullah, and Zheng Li. Pyod: A python toolbox for scalable outlier detection. *Journal of Machine Learning Research*, 20(96):1–7, 2019.
- [80] Songzhu Zheng, Pengxiang Wu, Aman Goswami, Mayank Goswami, Dimitris Metaxas, and Chao Chen. Error-bounded correction of noisy labels. In *ICML*, pages 11447–11457, 2020.